Climate Adjustment of Photosynthetically Active Radiation Estimates Using Site Adaptation Technique

Francisco Ferrera-Cobos[1], Ousmane Wane[1, 2], Ana A. Navarro[1], Cecilia Popovich[3], Gustavo H. Ribeiro da Silva[4], María Navarro Llorens[5], Luisa Gouveia[6, 7], Luis F. Zarzalejo[1] and Rita X. Valenzuela[1]

[1] CIEMAT Energy Department, Renewable Energy Division, Madrid (Spain)

[2] E.T.S.I. Agronómica, Alimentaria y Biosistemas, Universidad Politécnica de Madrid, Madrid (Spain)

[3] Laboratorio de Estudios Básicos y Biotecnológicos en Algas (LEBBA). Centro de Recursos Naturales Renovables de la Zona Semiárida (CERZOS) CONICET-UNS, Departamento de Biología, Bioquímica y Farmacia (UNS), Bahía Blanca (Argentina)

[4] Department of Environmental and Civil Engineering, São Paulo State University (UNESP), São Paulo (Brazil)

[5] Grupo de Ingeniería metabólica Departamento de Bioquímica y Biología Molecular, Universidad Complutense de Madrid, Madrid (Spain)

[6] LNEG UBB - Laboratório Nacional de Energia e Geologia IP. - Unidade de Bioenergia e Biorrefinarias, Lisboa, (Portugal)

[7] GreenCoLab - Green Ocean Technologies and Products Collaborative Laboratory, CCMAR, University of Algarve, Campus de Gambelas, Faro, (Portugal)

Abstract

In this work, a local adjustment is proposed for photosynthetically active radiation (PAR) estimates at several locations around the world with different Köppen-Geiger climate classes, resulting in a climate adjustment for PAR estimates. For adjustment, a site adaptation technique was used for each of the climates (hemiboreal, semi-arid, mediterranean, oceanic, and tropical) represented in this study. Remote sensing PAR data from thirteen locations were collected from the Copernicus CAMS global greenhouse gas reanalysis (EGG4) dataset to be used as initial PAR estimates, while observed PAR data from the same locations were also collected to perform the local adjustment. The results evidenced good fitting for four out of five climates; conversely, the semi-arid climate had to be divided into two subclimates (hot and cold semi-arid) to obtain good results. After division, the best results were obtained for the cold semi-arid and mediterranean climates. In the hot semi-arid climate, the results were contradictory, since it had the worst determination coefficient and the second-best MBE and RMSE among all climates. These results suggest that PAR is affected by local climatic and atmospheric conditions.

Keywords: Photosynthetically Active Radiation, PAR, Modelling

1. Introduction

Photosynthetically Active Radiation (PAR) is the portion of solar radiation whose wavelength is located between $4 \cdot 10^{-7}$ m and $7 \cdot 10^{-7}$ m. It is the range of the solar spectrum that plants use to perform photosynthesis, and it is the visible range for the human eye as well. PAR can be expressed as the photosynthetic photon flux density measured in µmol s^{-1} m^{-2} or as the energy flux density measured in W m^{-2}. In this work, the term PAR refers to the energy flux density and is expressed as W m^{-2}.

Despite its many applications, for example in estimating biomass growth or in calculating gross and primary production (Iasimone et al., 2018; Pinker et al., 2010; Trofimchuk et al., 2019; Wu et al., 2009), PAR is not as

Selection and/or peer review under responsibility of Scientific Committee
10.18086/eurosun.2024.10.03 Available at http://proceedings.ises.org

commonly measured as other solar components. When ground PAR data are not available, satellite-derived PAR estimates are a good option to consider because they usually cover long time periods and the entire surface of the world.

PAR is strongly dependent on local atmospheric and climatic conditions (Ferrera-Cobos et al., 2020a). Consequently, PAR models also depend on the data used to train the models. Previous studies addressed PAR modelling, analysing climatology and meteorological conditions (Ferrera-Cobos et al., 2020b; García-Rodríguez et al., 2021; Wang et al., 2021).

Site adaptation is a process in which the long-term time series of a modelled variable is improved in accuracy by using the short-term observations of the variable. It is often used when the variable is the irradiance or one of the components of the irradiance, employing mathematical adjustments to perform the site adaptation process (Ferrera-Cobos et al., 2020b; Mazorra Aguiar et al., 2019; Polo et al., 2016).

This work presents a climate adjustment for satellite-derived PAR estimates from 13 locations around the world, covering five different climates according to their Köppen-Geiger clasification. The adjustment was performed using a site adaptation technique.

2. Materials and Methods

Satellite-derived PAR data from 13 locations were collected from the Copernicus CAMS global greenhouse gas reanalysis (EGG4) (Agustí-Panareda et al., 2023) dataset from 2013 to 2020 along with ground PAR observations from the GEOPAR network, AMERIFLUX (Yepez, 2020), CERZOS CONICET-UNS, São Paulo State University and Helsinki University-Viikki Campus (https://osf.io/e4vau/), overlapping at least one year in that time span from the same 13 locations. The daily average was calculated for both data sets.

Thirteen locations, covering five climates according to the Köppen-Geiger climate classification (hemiboreal climate, semi-arid climate, mediterranean climate, oceanic climate, and tropical climate), provided PAR ground data. More details of each location can be found in the Tab. 1. Tropical (Aw) and subtropical (Cfa) climates were combined into a single class named tropical, while the climate subgroup Bsks was classified as a Mediterranean climate.

For local climate adjustment, this work used a site adaptation technique for each of the climates represented in this study. Site adaptation consisted of a fitting between remote sensing data and observed data. In this case, satellite-derived PAR estimates were fitted using ground-observed PAR data from the radiometric stations listed in Tab. 1 and Fig. 1.

Tab. 1. Locations. Positive degrees indicate north latitude or east longitude.

Country	Location	Latitude	Longitude	Altitude (m)	Köppen-Geiger classification	Climate type
Spain	Tabernas	37.092	-2.364	491	Bskw	Semiarid
México	Alamos	26.997	-108.789	367	Bsh	Semiarid
Spain	Albacete	39.041	-2.082	698	Bsks	Mediterranean
Spain	Salamanca	40.978	-5.715	777	Bsks	Mediterranean
Spain	Lubia	41.601	-2.508	1099	Bsks	Mediterranean
Spain	Córdoba	37.857	-4.803	91	Csa	Mediterranean
Spain	Zaragoza	41.727	-0.814	226	Bsks	Mediterranean
Spain	Lugo	42.995	-7.541	447	Csb	Oceanic
Spain	Villaviciosa	43.476	-5.441	6	Cfb	Oceanic
Spain	Vitoria	42.854	-2.622	520	Csb	Oceanic
Argentina	Bahía Blanca	-38.678	-62.232	42	Cfa	Tropical
Brasil	Baurú	-22.351	-49.033	610	Aw	Tropical
Finland	Helsinki	60.225	25.017	8	Dfb	Hemiboreal

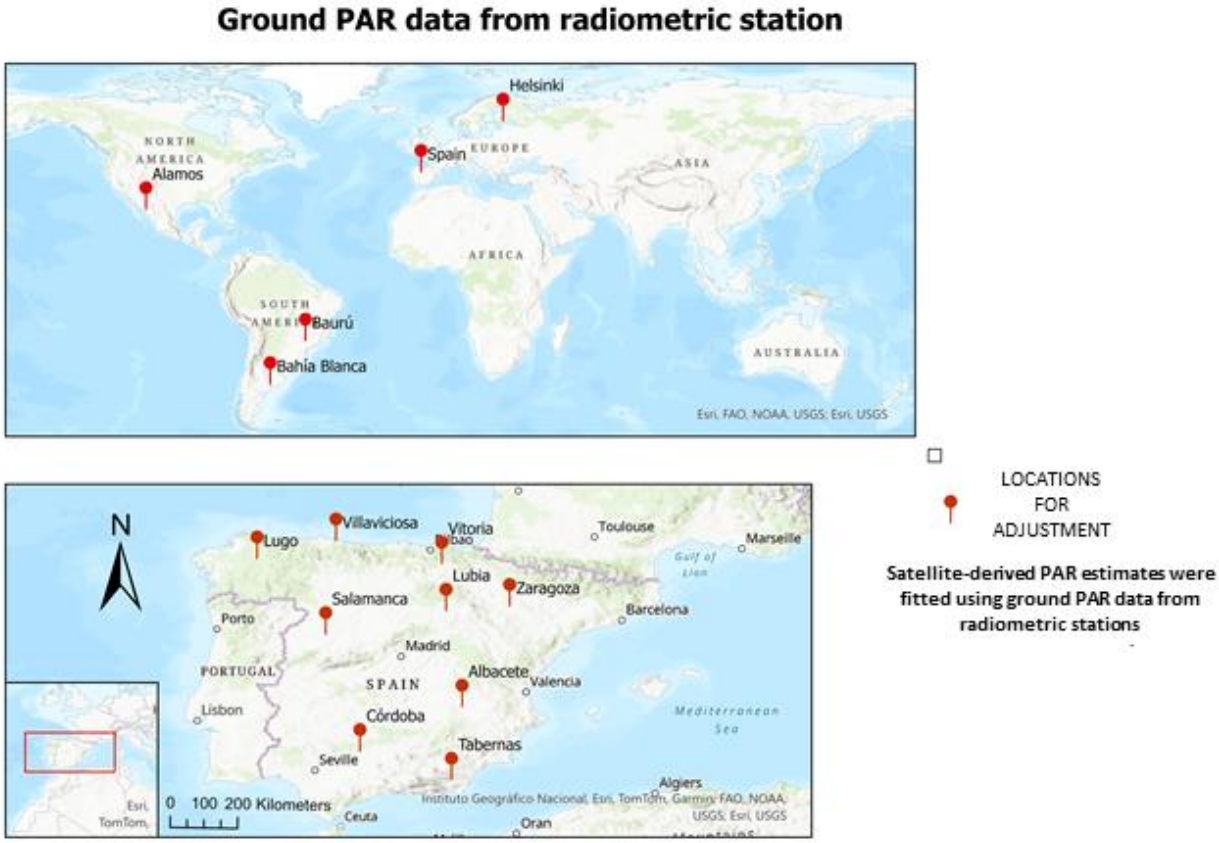

Fig. 1. Locations used in this work.

All data from the 13 locations were classified according to their Köppen-Geiger class. As there were some similar climate classes, the climatic classification was simplified into the following five groups.

- Hemiboreal
- Semi-arid
- Mediterranean
- Oceanic
- Tropical

A linear regression between the PAR satellite-derived data and the PAR ground observations was used to perform site adaptation for each of the climates, as illustrated in eq. 1. This method implies the use of observed data to refine satellite estimates.

$$y_{local} = a \cdot x_{satellite} + b \qquad \text{(eq. 1)}$$

Where the slope of the linear regression is a, the intercept is b, y_{local} refers to the ground-observed data, $x_{satellite}$ indicates the satellite-derived data.

In this work, this methodology is applied to PAR data. Therefore, the ground-observed PAR data is used as y_{local}, whereas the satellite-derived PAR data is used as $x_{satellite}$. To perform the training of the models, the fittings were conducted for each of the groups of PAR data (hemiboreal climate, semiarid climate, mediterranean climate, oceanic climate, and tropical climate) allowing us to obtain the corresponding parameters a and b for each of the climates. These parameters can be used to estimate PAR in a location with the same climate, using PAR satellite-derived data from this location, as eq. 2 shows. Thus, using eq. 2 we can obtain local climate-based PAR estimates from satellite-derived data.

The mathematical expression of the resulting PAR model derived from the linear regressions is shown in eq. 2.

$$PAR_{adjusted} = a \cdot PAR_{satellite} + b \qquad \text{(eq. 2)}$$

To eliminate outliers, the data were previously checked and filtered. Any data whose ratio between ground-observed PAR and satellite-derived PAR differed more than 40% from the mean of the dataset ratio were dismissed.

The corresponding PAR data for each of the climates were randomly divided 70/30 into two groups. The first group, which contained 70% of the data, was used to train the models and obtain the parameters a and b for each climate. The remaining data were subsequently used to validate the models.

3. Results

The preliminary results training the models showed good correlations in all climates except in the semi-arid case, where the R^2 was 0.563. Furthermore, two different data groups can be observed in Fig. 2, since the scatterplot between the measured and remote-sensing PAR shows a 'V' shape. As a consequence, semi-arid climate was divided into two subclasses: Cold Semi-arid and Hot Semi-arid. After division, the R^2 numbers improved significantly, from 0.563 to 0.918 and 0.801, respectively. The statistics MBE (mean bias error) and RMSE (root mean squared error) improved as well in the cold semi-arid climate. In contrast, these statistics showed worse numbers in the hot semi-arid climate. Interestingly, the slopes obtained differ significantly from the cold to the hot semi-arid climate (1.20 to 1.67).

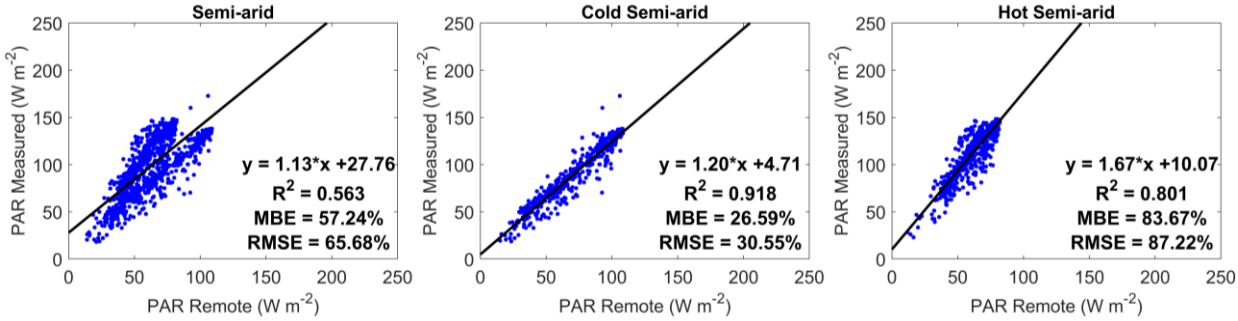

Fig. 2. Training models for semi-arid climates

Fig. 3 illustrates the results of training the models, with the semi-arid climate divided into two subclasses.

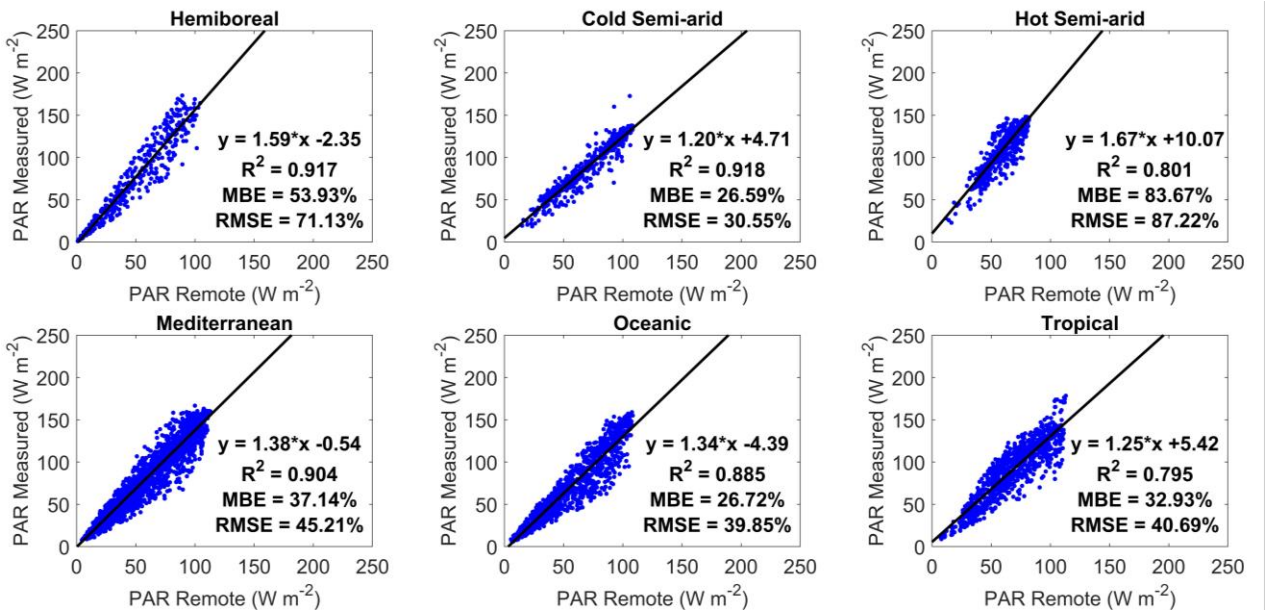

Fig. 3. Results of the training process for each climate.

Interestingly, all climates showed good correlations, the worst being tropical, where the R^2 was 0.795. Although MBE and RMSE did not show numbers lower than 26%. It is also noticeably that the slopes vary from one climate to another; the highest slope is for the hot semi-arid climate, and the lowest slope is for the cold semi-arid climate. The remaining slopes range between these two extremes. Thus, according to these results, the model adjustment for each climate is illustrated in Tab. 2.

Tab. 2. Model expressions for each climate.

Climate type	Model expression
Hemiboreal	$PAR = 1.59 \cdot PAR_{satellite} - 2.35$
Cold Semi-arid	$PAR = 1.20 \cdot PAR_{satellite} + 4.71$
Hot Semi-arid	$PAR = 1.67 \cdot PAR_{satellite} + 10.07$
Mediterranean	$PAR = 1.38 \cdot PAR_{satellite} - 0.54$
Oceanic	$PAR = 1.34 \cdot PAR_{satellite} - 4.39$
Tropical	$PAR = 1.25 \cdot PAR_{satellite} + 5.42$

The expressions for the adjusted models were validated using the remaining 30% of the data that were not used in the training process. Fig. 4 shows the validation results.

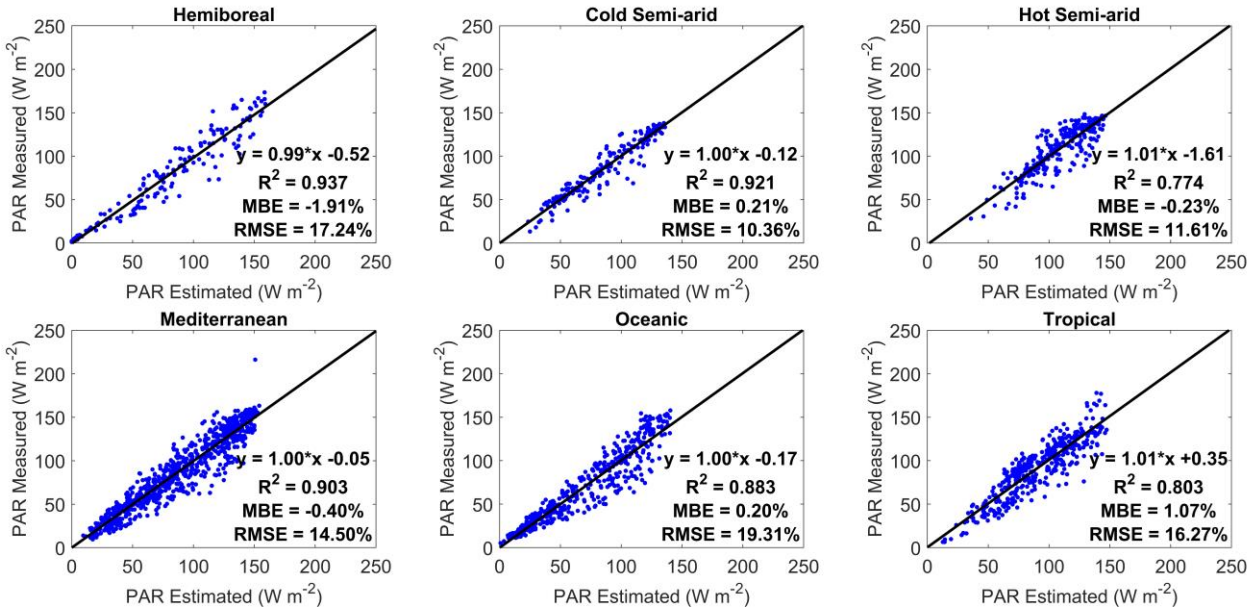

Fig. 4. Results of the validation process for each climate.

The results indicate a good performance of the models, as all slopes range from 0.99 to 1.01, and a good determination coefficient, as the lowest R2 is 0.774 and three of them are above 0.9. The MBE in absolute value is below 2% in all cases. However, the worst statistics obtained were RMSE, which in no case was lower than 10%. Model adjustment seems to perform better in dry and stable weather climates such as cold semi-arid or Mediterranean climates. Models obtained worse results in climates where precipitations are more common, such as tropical or oceanic. Interestingly, the error statistics in the hot semi-arid climate are good, despite having the worst R^2. In fact, its MBE and RMSE (-0.23% and 11.61%, respectively) are the second lowest among all climates under study. This climate is only covered by one location, thus local perturbations or disturbances cannot be ruled out, and further research is needed to understand and improve the model adjustment in this climate.

4. Conclusions

A local adjustment was proposed for photosynthetically active radiation (PAR) estimates in 13 locations around the world with five different climate types. The proposed methodology develops local models using satellite-derived and ground-observed PAR data. Merging data from sites with the same climatic features enable to develop models based on their climatic classification. Therefore, these models can also be used to estimate PAR in other locations whose climate is the same. The estimates provided by the proposed models are a useful tool for obtaining PAR data at locations where no ground observed data are available and can be of interest for energy balance in ecosystem calculations, biomass production models, agrofood industry, etc. that need PAR data as input.

The statistical results showed a good correlation between the adjusted satellite-derived PAR estimates using the proposed method and the ground-measured PAR data at the locations studied. The type of semi-arid climate initially showed a poor correlation; indeed, two groups of data could be observed. This made it necessary to divide the semiarid climate type into two classes (hot semiarid and cold semiarid) to obtain good fitting results, supporting the idea that PAR is strongly dependent on local climatic and atmospheric conditions. The best results were obtained for the cold semi-arid and mediterranean climates. This good performance of the models in the cold semi-arid and mediterranean climates was expected, as both are usually dry and stable weather climates, so that the satellite-derived estimates are normally more accurate and so does the model adjustment proposed. Noticeably, the results in the hot semi-arid climate are shocking. On the one hand, it had the worst determination coefficient among all climates, and nevertheless its MBE and RMSE are the second best. This could be explained due to local disturbances as this climate is only covered by one location. These results suggest that PAR is affected by local atmospheric conditions, and further research in this field is needed.

5. Acknowledgements

This research was funded by the Spanish Ministry of Science and Innovation (MCIN/AEI/10.13039/501100011033) and the European Union ‘Next Generation EU”/PRTR, TEDDY (TED2021-130366B-I00). The authors also acknowledge the CYTED-Ibero American Programme on Science and Technology for Development (RED RENUWAL P320RT0005 CYTED). Satellite data were downloaded from the Copernicus Atmosphere Monitoring Service (CAMS) Atmosphere Data Store (ADS), particularly global greenhouse gas reanalysis (EGG4) (https://ads.atmosphere.copernicus.eu/cdsapp#!/dataset/cams-global-ghg-reanalysis-egg4?tab=overview) (accessed in February 2022). We acknowledge the following AmeriFlux sites for their data records: MX-Aog (Alamos). In addition, funding for AmeriFlux data resources was provided by the U.S. Department of Energy’s Office of Science. The authors also acknowledge Dr. Pedro Aphalo for the Viikki (Helsinki) PAR data.

6. References

Ferrera-Cobos, F., Vindel, J.M., Valenzuela, R.X., González, J.A., 2020a. Analysis of Spatial and Temporal Variability of the PAR/GHI Ratio and PAR Modeling Based on Two Satellite Estimates. Remote Sens (Basel) 12, 1262. https://doi.org/10.3390/rs12081262

Ferrera-Cobos, F., Vindel, J.M., Valenzuela, R.X., González, J.A., 2020b. Models for estimating daily photosynthetically active radiation in oceanic and mediterranean climates and their improvement by site adaptation techniques. Advances in Space Research 65, 1894–1909. https://doi.org/10.1016/j.asr.2020.01.018

García-Rodríguez, A., Granados-López, D., García-Rodríguez, S., Díez-Mediavilla, M., Alonso-Tristán, C., 2021. Modelling Photosynthetic Active Radiation (PAR) through meteorological indices under all sky conditions. Agric For Meteorol 310, 108627. https://doi.org/10.1016/j.agrformet.2021.108627

Iasimone, F., Panico, A., De Felice, V., Fantasma, F., Iorizzi, M., Pirozzi, F., 2018. Effect of light intensity and nutrients supply on microalgae cultivated in urban wastewater: Biomass production, lipids accumulation and settleability characteristics. J Environ Manage 223, 1078–1085. https://doi.org/10.1016/j.jenvman.2018.07.024

Mazorra Aguiar, L., Polo, J., Vindel, J.M., Oliver, A., 2019. Analysis of satellite derived solar irradiance in islands with site adaptation techniques for improving the uncertainty. Renew Energy 135, 98–107. https://doi.org/10.1016/j.renene.2018.11.099

Pinker, R.T., Zhao, M., Wang, H., Wood, E.F., 2010. Impact of satellite based PAR on estimates of terrestrial net primary productivity. Int J Remote Sens 31, 5221–5237. https://doi.org/10.1080/01431161.2010.496474

Polo, J., Wilbert, S., Ruiz-Arias, J.A., Meyer, R., Gueymard, C., Súri, M., Martín, L., Mieslinger, T., Blanc, P., Grant, I., Boland, J., Ineichen, P., Remund, J., Escobar, R., Troccoli, A., Sengupta, M., Nielsen, K.P., Renne, D., Geuder, N., Cebecauer, T., 2016. Preliminary survey on site-adaptation techniques for satellite-derived and reanalysis solar radiation datasets. Solar Energy 132, 25–37. https://doi.org/10.1016/j.solener.2016.03.001

Trofimchuk, O.A., Petikar, P. V., Turanov, S.B., Romanenko, S.A., 2019. The influence of PAR irradiance on yield growth of Chlorella microalgae. IOP Conf Ser Mater Sci Eng 510. https://doi.org/10.1088/1757-899X/510/1/012017

Wang, C., Du, J., Liu, Y., Chow, D., 2021. A climate-based analysis of photosynthetically active radiation availability in large-scale greenhouses across China. J Clean Prod 315, 127901. https://doi.org/10.1016/j.jclepro.2021.127901

Wu, C., Niu, Z., Tang, Q., Huang, W., Rivard, B., Feng, J., 2009. Remote estimation of gross primary production in wheat using chlorophyll-related vegetation indices. Agric For Meteorol 149, 1015–1021. https://doi.org/10.1016/j.agrformet.2008.12.007

Yepez, E.A., 2020. AmeriFlux BASE MX-Aog Alamos Old-Growth tropical dry forest, Ver. 1-5, AmeriFlux AMP, (Dataset). https://doi.org/10.17190/AMF/1756414